

# BEC-BCS crossover driven by the axial anomaly in the NJL model

Hiroaki Abuki\*, Gordon Baym†, Tetsuo Hatsuda\*\* and Naoki Yamamoto‡

\**Department of Physics, Tokyo University of Science, Tokyo 162-8601, Japan*

†*Department of Physics, University of Illinois, 1110 W. Green St., Urbana, Illinois 61801, USA*

\*\**Department of Physics, The University of Tokyo, Tokyo 113-0033, Japan*

‡*Institute for Nuclear Theory, University of Washington, Seattle, WA 98195-1550, USA*

**Abstract.** We study the QCD phase structure in the three-flavor Nambu–Jona-Lasinio model, incorporating the chiral-diquark interplay due to the axial anomaly. We demonstrate that for a certain range of model parameters, the low temperature critical point predicted by a Ginzburg-Landau analysis appears in the phase diagram. In addition, we show that the axial anomaly presents a new scenario for a possible BEC-BCS crossover in the color-flavor locked phase of QCD.

**Keywords:** QCD, quark matter, superconducting, Bose-Einstein condensate

**PACS:** 12.38.-t, 25.75.Nq

## INTRODUCTION

The phases of QCD at finite temperature  $T$  and quark chemical potential  $\mu$  are being actively studied. In particular, at low  $T$  and high  $\mu$  a color superconducting (CSC) phase [1, 2] characterized by a diquark condensate  $\langle qq \rangle$  is expected to appear owing to the attractive interaction between quarks, provided either by one-gluon exchange or by instantons. On the other hand, when the system at finite  $\mu$  is heated, a transition to a quark-gluon plasma (QGP) takes place at a (pseudo-)critical temperature.

Our understanding of the phase structure based on the lattice simulations is still immature due to the severe sign problem at finite  $\mu$ . Therefore the analyses so far have relied mainly on specific models of QCD, such as the Nambu–Jona-Lasinio model [3, 4], the Polyakov–Nambu–Jona-Lasinio (PNJL) model [5], and etc. Some of these model indicated the possible existence of a critical point located at high  $T$  [6].

The interesting possibility of a second critical point at rather low temperature in the color-flavor locked (CFL) phase was recently predicted on the basis of general Ginzburg-Landau (GL) analysis [7]. Moreover, this critical point has proven to make a quark-hadron continuity possible [8, 9, 10]. In two-flavor QCD, similar critical points have been found in the NJL model [11], although their origin is different from axial anomaly.

This work is aimed at locating this critical point in the  $(\mu, T)$ -phase diagram using the phenomenological NJL model [12]. Starting with the three-flavor NJL model incorporating the axial anomaly induced chiral-diquark interplay, we study the location of the new critical point and its dependence on the strength of the anomaly. We also observe that the axial anomaly triggers a crossover between a Bose-Einstein condensed state (BEC) of diquark pairing and Bardeen-Cooper-Schrieffer (BCS) diquark pairing [13, 14, 15, 16, 17] in the CFL phase.

## INCORPORATING THE AXIAL ANOMALY IN NJL MODEL

The Lagrangian of the NJL model with three-flavors consists of three terms:

$$\mathcal{L} = \bar{q}(i\gamma_\mu \partial^\mu - m_q + \mu\gamma_0)q + \mathcal{L}^{(4)} + \mathcal{L}^{(6)}, \quad (1)$$

where  $q = (u, d, s)$  is the flavor triplet quark field,  $m_q$  is a flavor symmetric quark mass ( $m_u = m_d = m_s$ ), and  $\mu$  is the chemical potential for conserved quark number.  $\mathcal{L}^{(4)}$  and  $\mathcal{L}^{(6)}$  are the four-fermion and six-fermion interactions, respectively. As usual we set  $\mathcal{L}^{(4)} = \mathcal{L}_\chi^{(4)} + \mathcal{L}_d^{(4)}$  with the standard choice [3, 4]

$$\mathcal{L}_\chi^{(4)} = 8G\text{tr}(\phi^\dagger \phi), \quad \mathcal{L}_d^{(4)} = 2H\text{tr}[d_L^\dagger d_L + d_R^\dagger d_R], \quad (2)$$

where  $\phi_{ij} \equiv (\bar{q}_R)_a^j (q_L)_a^i$ ,  $(d_L)_{ai} \equiv \epsilon_{abc} \epsilon_{ijk} (q_L)_b^j C (q_L)_c^k$ , and  $(d_R)_{ai} \equiv \epsilon_{abc} \epsilon_{ijk} (q_R)_b^j C (q_R)_c^k$ , with  $a, b, c$  and  $i, j, k$  the color and flavor indices, and  $C$  the charge conjugation operator. The flavor  $U(3)$  generators  $\tau_a$  ( $a = 0, \dots, 8$ ) are normalized so that  $\text{tr}[\tau_a \tau_b] = 2\delta_{ab}$ , and  $\tau_A$  and  $\lambda_{A'}$  with  $A, A' = 2, 5, 7$  are antisymmetric generators of flavor and  $SU(3)$  color, respectively.  $\mathcal{L}^{(4)}$  is invariant under  $SU(3)_L \times SU(3)_R \times U(1)_A \times U(1)_B$  symmetry. The interaction  $\mathcal{L}_\chi^{(4)}$  produces attraction of  $q\bar{q}$  pairs, leading to the formation of a chiral condensate. Similarly  $\mathcal{L}_d^{(4)}$  leads to attraction of  $qq$  pairs in the color-anti-triplet and spin-parity  $0^\pm$  channel, inducing a color-flavor locked (CFL) condensate [1]. We treat the two couplings  $G$  and  $H$  as independent parameters.

The six-fermion interaction in our model consists of two parts,  $\mathcal{L}^{(6)} = \mathcal{L}_\chi^{(6)} + \mathcal{L}_{\chi d}^{(6)}$ .  $\mathcal{L}_\chi^{(6)}$  is the standard Kobayashi-Maskawa-'t Hooft (KMT) interaction [18],

$$\mathcal{L}_\chi^{(6)} = -8K (\det \phi + \text{h.c.}). \quad (3)$$

This interaction is not invariant under  $U(1)_A$  symmetry, which accounts for the axial anomaly in QCD due to instantons. Consequently the mass of the  $\eta'$  meson becomes larger than that of the other pseudoscalar octet Nambu-Goldstone (NG) bosons ( $\pi, \eta, K$ ) for positive value of  $K$ . On the other hand, the term (3) makes the chiral phase transition first-order as a function of  $T$  at  $\mu = 0$  for the massless three-flavor limit [19].

As shown in [7], the instanton can induce a coupling between the chiral and diquark condensates through a new six-fermion term:

$$\mathcal{L}_{\chi d}^{(6)} = K' \left( \text{tr}[(d_R^\dagger d_L) \phi] + \text{h.c.} \right). \quad (4)$$

It is this term that is responsible for the aforementioned low temperature critical point. We assume  $K' > 0$ , so that  $qq$  pairs in the positive parity channel,  $\langle d_L \rangle = -\langle d_R \rangle$ , are energetically favored. We keep  $K$  and  $K'$  as independent parameters [12].

The condensates favored by the interaction  $\mathcal{L}^{(4)} + \mathcal{L}^{(6)}$  are the flavor-symmetric chiral and diquark condensates in the spin-parity  $0^+$  channel, defined by

$$\langle \phi_{ij} \rangle = (\chi/2)\delta_{ij}, \quad \langle d_{Lai} \rangle = -\langle d_{Rai} \rangle = (s/2)\delta_{ai}. \quad (5)$$

**TABLE 1.** Two sets of parameters in the present three-flavor NJL model: The momentum cutoff is fixed at  $\Lambda = 602.3$  MeV [4]. The dynamical quark mass  $M$  and the chiral condensate  $\chi$  at vacuum are also given.

	$m_q$ [MeV]	$G\Lambda^2$	$H\Lambda^2$	$K\Lambda^5$	$M$ [MeV]	$\chi^{1/3}$ [MeV]
Set I	0	1.926	1.74	12.36	355.2	-240.4
Set II	5.5	1.918	1.74	12.36	367.6	-241.9

Here the condensate order parameters are  $\chi$  and  $s$ .

It is straightforward to derive the thermodynamic potential at the mean-field level [12]

$$\begin{aligned} \Omega(\chi, s; \mu, T) = & U(\chi, s) - \int_{|p| \leq \Lambda} \frac{d^3 p}{(2\pi)^3} \sum_{\pm} [8\omega_8^{\pm} + \omega_1^{\pm}] \\ & - 2T \int \frac{d^3 p}{(2\pi)^3} \sum_{\pm} \left[ 8 \ln(1 + e^{-\omega_8^{\pm}/T}) + \ln(1 + e^{-\omega_1^{\pm}/T}) \right], \end{aligned} \quad (6)$$

where  $\Lambda$  is a momentum cutoff to regulate the vacuum energy,

$$U(\chi, s) = 6G\chi^2 + 3H|s|^2 - 4K\chi^3 - \frac{3}{2}K'|s|^2\chi, \quad (7)$$

is a constant term which is needed to cancel double counting of the interactions, and

$$\omega_8^{\pm} = \sqrt{(\sqrt{M^2 + p^2} \pm \mu)^2 + (2\Delta)^2}, \quad \omega_1^{\pm} = \sqrt{(\sqrt{M^2 + p^2} \pm \mu)^2 + \Delta^2} \quad (8)$$

are the dispersion relations for the quasi-quarks in the octet and singlet representations, with  $M$  and  $\Delta$  the dynamical Dirac and Majorana masses, defined as

$$M = m_q - 4 \left( G - \frac{1}{2}K\chi \right) \chi + \frac{1}{4}K'|s|^2, \quad \Delta = -2 \left( H - \frac{1}{4}K'\chi \right) |s|. \quad (9)$$

These equations imply that  $\chi < 0$  is energetically favored for non-zero  $m_q$ , while  $s$  is generally complex; the thermodynamic potential is a function of  $|s|^2$ .

## PHASE STRUCTURE AND DISCUSSION

The phase structures can be determined numerically by looking for the values of  $\chi$  and  $s$  that minimize the thermodynamic potential in Eq. (6). We follow the parameter choice of [4]. We show in Table 1 two sets of parameters we adopt, Set I and Set II respectively. We vary the strength of the chiral-diquark coupling (the  $K'$  term) by hand. We work in the flavor SU(3) limit, assuming  $m_u = m_d = m_s \equiv m_q$  for simplicity.

We show in Fig. 1 the phase structures for Set I (massless case) in the upper panel, and those for Set II (massive case) in the lower panel. Panels (a) and (b) show the results without and with the  $K'$ -term; in (b) we have taken  $K' = 4.2K_0$  with  $K_0 = 12.36/\Lambda^5$  as

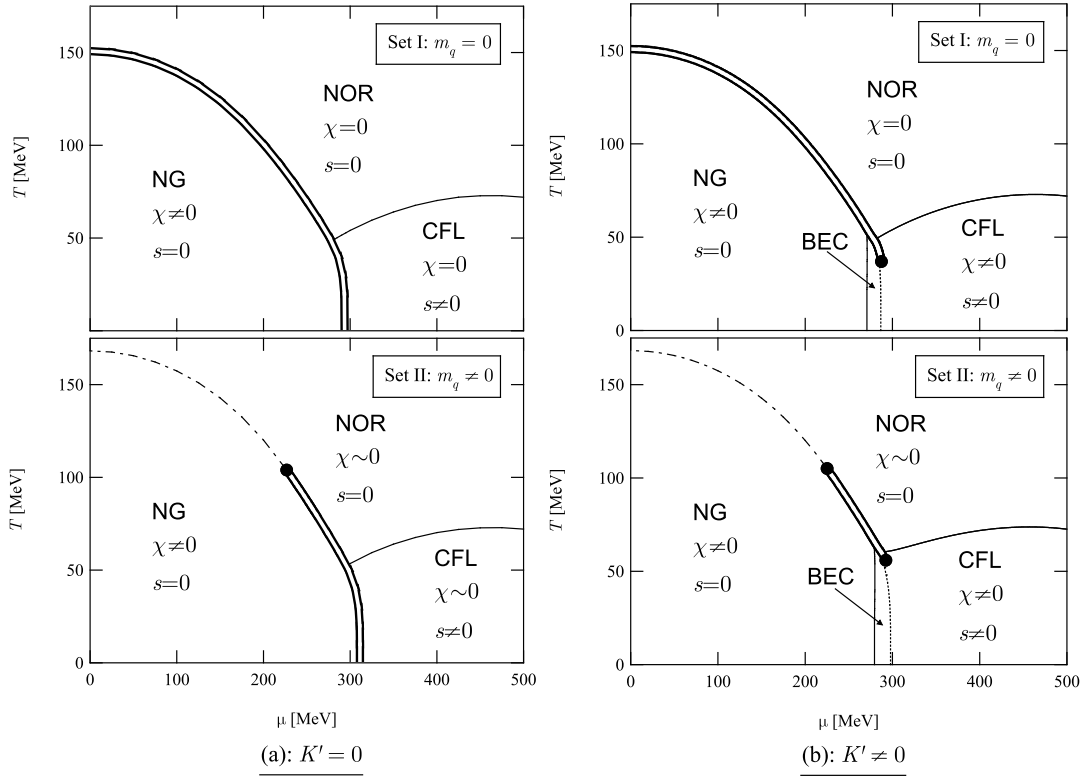


**FIGURE 1.** The phase structure in the  $(\mu, T)$ -plane in the three-flavor NJL model without (a) and with (b) the  $K'$  term. The Upper and lower panels present the results in the massless case I and the massive case II respectively. Phase boundaries with a second-order transition are denoted by a single line and a first-order transition by a double line. The dashed-dot line at high T in case II shows the chiral crossover line, while the dotted line in (b) denotes the BEC-BCS crossover. See [12] for further details.

a representative value. The phase diagrams contain a CFL phase with  $s \neq 0$  with  $U(1)$  baryon number broken, and other two phases both characterized with  $s = 0$ , a Nambu-Goldstone (NG) phase with  $\chi \neq 0$  and a normal (NOR) phase with either  $\chi = 0$  (in case  $m_q = 0$ ) or  $\chi \sim 0$  (in case  $m_q \neq 0$ ). From the two figures in the panel (a), we see that the current quark mass leads to the critical point on the high temperature side of the first-order line of chiral phase transition [6]. The critical point moves downwards with increasing quark mass  $m_q$  since it acts as an external symmetry breaking source of chiral symmetry breaking and thus smears the strength of the phase transition.

The effect of nonvanishing  $K'$  can be seen by comparing (a) and (b). We indeed see that the low temperature critical point shows up at the other end of the line of the first order chiral phase transition. This is, as discussed in [7], because the  $K'$ -term acts as an external field for  $\chi$ , which turns the first-order chiral phase transition into a crossover in the CFL phase where  $s \neq 0$ . Note that the CFL phase in the panel (b) accompanies a nonzero chiral condensate  $\chi \neq 0$  induced by the anomaly mixing term  $\mathcal{L}_{\chi d}^{(6)}$ .

The axial anomaly, for sufficiently large chiral-diquark coupling  $K'$ , not only triggers the low  $T$  critical point, but also drives a BEC-BCS crossover in the CFL phase, as discussed in [17]. Within an NJL-type model such a BEC regime appears for sufficiently

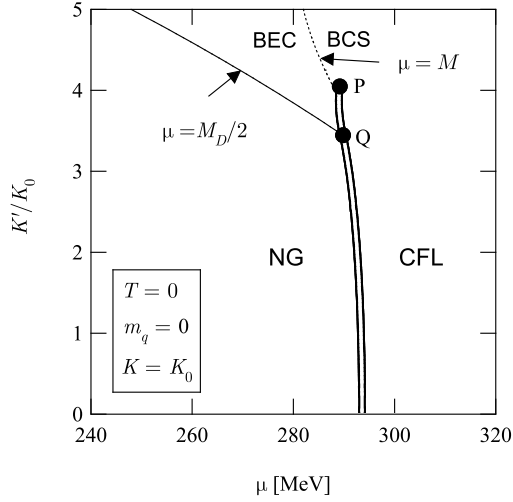


**FIGURE 2.** The phase diagram in the  $(\mu, K')$ -plane at  $T = 0$  for massless quarks, with the NG and CFL phases. A dotted line separates the CFL phase into BCS- and BEC-like domains. The critical point and the critical end point are denoted by P and Q, respectively.

large pairing attraction,  $H$ , in the  $qq$ -channel [14, 15, 16]. The novel feature here is that the axial anomaly helps to realize the BEC regime through its contribution to the effective  $qq$  coupling. This can be easily seen by extracting from Eq. (4) the dominant zero mode ( $\phi_{ij} \sim \delta_{ij}\chi/2$ ) contribution to the quark-quark interaction

$$\mathcal{L}_{\chi d}^{(6)} \sim \frac{1}{4}K'|\chi|\text{tr}[(d_R - d_L)^\dagger(d_R - d_L)] - \frac{1}{4}K'|\chi|\text{tr}[(d_R + d_L)^\dagger(d_R + d_L)]. \quad (10)$$

The first term increases the effective attraction between quarks in the  $0^+$  channel, while the second term is repulsive and suppresses the  $0^-$  pairing. Thus when the chiral condensate is nonvanishing, as in the NG phase, the axial anomaly helps the formation of a diquark BEC condensate.

In fact it is possible to show that at sufficiently large  $K'$  there are nine diquark bound states with mass  $M_D(\mu, T) \leq 2M(\mu, T)$  where  $M(\mu, T)$  is the dynamical Dirac mass of quarks at  $\mu$  and  $T$ . Each diquark complex scalar has quark number  $\pm 2$  so that it feels chemical potential  $2\mu$ . Thus when  $2\mu$  hits  $M_D(\mu, T)$  from below a BEC condensate must start to form. Then the condition for the onset of a BEC approaching from the NG phase (NG-BEC boundary) is given by the condition [20, 14]

$$2\mu = M_D(\mu, T). \quad (11)$$

In order to see how the BEC domain in the CFL phase grows as a function of  $K'$ , we show in Fig. 2 the phase diagram in the  $(\mu, K')$ -plane for massless quarks. The first-order line separating the CFL and NG phases for small  $K'$  eventually terminates at the critical point P. On the other hand, for  $K'$  sufficiently large, a BEC regime of bound diquarks appears across a second-order phase transition at a critical chemical potential  $\mu = M_D(\mu, 0)/2$  shown by solid line; the phase boundary meets the first-order line at the critical end point Q. A novel first-order transition from the BEC to BCS regimes

appears between P and Q, with discontinuous changes of both the chiral and diquark condensates.

In conclusion, the axial anomaly, by driving a coupling between the chiral and diquark condensates, plays an important role in the many body physics of QCD, making the phase diagram extremely rich. For one, we demonstrated that it can indeed produce the low temperature critical point between the hadronic phase and the color superconducting phase predicted by the previous GL analysis [7]. In addition, we have shown that the coupling helps the formation of a BEC of diquarks via increasing effective quark-quark attraction in the  $0^+$  channel. As a result, a BEC-BCS crossover or even the first order BEC-BCS transition can be realized in the CFL phase.

Finally we note that very recently the extension of our analysis incorporating the effect of heavy strange quark mass was reported [21]. It still remains an important task to extend the analyses imposing the charge neutrality and  $\beta$ -equilibrium conditions.

The numerical calculations were carried out on Altix3700 at YITP in Kyoto University.

## REFERENCES

1. K. Rajagopal and F. Wilczek, arXiv:hep-ph/0011333; D. H. Rischke, Prog. Part. Nucl. Phys. **52**, 197 (2004); M. G. Alford, A. Schmitt, K. Rajagopal and T. Schafer, Rev. Mod. Phys. **80**, 1455 (2008).
2. K. Fukushima and T. Hatsuda, arXiv:1005.4814 [hep-ph].
3. T. Hatsuda and T. Kunihiro, Phys. Rept. **247**, 221 (1994).
4. M. Buballa, Phys. Rept. **407**, 205 (2005).
5. K. Fukushima, Phys. Lett. B **591**, 277 (2004); C. Ratti, M. A. Thaler and W. Weise, Phys. Rev. D **73**, 014019 (2006); S. Roessner, C. Ratti and W. Weise, Phys. Rev. D **75**, 034007 (2007); H. Abuki, M. Ciminale, R. Gatto, G. Nardulli and M. Ruggieri, Phys. Rev. D **77**, 074018 (2008) [arXiv:0802.2396 [hep-ph]]; H. Abuki, R. Anglani, R. Gatto, G. Nardulli and M. Ruggieri, Phys. Rev. D **78**, 034034 (2008) [arXiv:0805.1509 [hep-ph]].
6. M. Asakawa and K. Yazaki, Nucl. Phys. A **504** (1989) 668; A. Barducci, R. Casalbuoni, S. De Curtis, R. Gatto and G. Pettini, Phys. Lett. B **231**, 463 (1989).
7. T. Hatsuda, M. Tachibana, N. Yamamoto and G. Baym, Phys. Rev. Lett. **97**, 122001 (2006).
8. T. Schafer and F. Wilczek, Phys. Rev. Lett. **82**, 3956 (1999) [arXiv:hep-ph/9811473].
9. N. Yamamoto, M. Tachibana, T. Hatsuda and G. Baym, Phys. Rev. D **76**, 074001 (2007); T. Hatsuda, M. Tachibana and N. Yamamoto, Phys. Rev. D **78**, 011501 (2008).
10. N. Yamamoto, JHEP **0812**, 060 (2008).
11. M. Kitazawa, T. Koide, T. Kunihiro and Y. Nemoto, Prog. Theor. Phys. **108**, 929 (2002).
12. H. Abuki, G. Baym, T. Hatsuda and N. Yamamoto, Phys. Rev. D **81**, 125010 (2010) [arXiv:1003.0408 [hep-ph]].
13. H. Abuki, T. Hatsuda and K. Itakura, Phys. Rev. D **65**, 074014 (2002) [arXiv:hep-ph/0109013].
14. Y. Nishida and H. Abuki, Phys. Rev. D **72**, 096004 (2005) [arXiv:hep-ph/0504083]; H. Abuki, Nucl. Phys. A **791**, 117 (2007) [arXiv:hep-ph/0605081].
15. L. He and P. Zhuang, Phys. Rev. D **75**, 096003 (2007); L. He and P. Zhuang, Phys. Rev. D **76**, 056003 (2007); L. He, arXiv:1007.1920 [hep-ph]; J. c. Wang, Q. Wang and D. H. Rischke, arXiv:1008.4029 [nucl-th].
16. M. Kitazawa, D. H. Rischke and I. A. Shovkovy, Phys. Lett. B **663**, 228 (2008).
17. G. Baym, T. Hatsuda, M. Tachibana and N. Yamamoto, J. Phys. G **35**, 104021 (2008).
18. M. Kobayashi and T. Maskawa, Prog. Theor. Phys. **44** (1970) 1422; G. 't Hooft, Phys. Rev. Lett. **37**, 8 (1976); Phys. Rev. D **14**, 3432 (1976) [Erratum-ibid. D **18**, 2199 (1978)].
19. R. D. Pisarski and F. Wilczek, Phys. Rev. D **29**, 338 (1984).
20. P. Nozières and S. Schmitt-Rink, J. Low. Temp. Phys. **59** 195 (1985).
21. H. Basler and M. Buballa, arXiv:1007.5198 [hep-ph].